Biomaterials and Biosystems 8 (2022) 100067

Contents lists available at ScienceDirect

Biomaterials and Biosystems

journal homepage: www.elsevier.com/locate/bbiosy

Human endothelial cells form an endothelium in freestanding collagen hollow filaments fabricated by direct extrusion printing

Ina Prade[a,*], Michaela Schröpfer[a], Caroline Seidel[a], Claudia Krumbiegel[a], Tina Hille[a], Frank Sonntag[b], Stephen Behrens[b], Florian Schmieder[b], Birgit Voigt[a], Michael Meyer[a]

[a] FILK Freiberg Institute, Meissner Ring 1-5, 09599 Freiberg, Germany
[b] Fraunhofer Institute of Materials and Beam Technology IWS, Winterbergstr. 28, 01277 Dresden, Germany

A B S T R A C T

Fiber-shaped materials have great potential for tissue engineering applications as they provide structural support and spatial patterns within a three-dimensional construct. Here we demonstrate the fabrication of mechanically stable, meter-long collagen hollow filaments by a direct extrusion printing process. The fibres are permeable for oxygen and proteins and allow cultivation of primary human endothelial cells (ECs) at the inner surface under perfused conditions. The cells show typical characteristics of a well-organized EC lining including VE-cadherin expression, cellular response to flow and ECM production. The results demonstrate that the collagen tubes are capable of creating robust soft tissue filaments. The mechanical properties and the biofunctionality of these collagen hollow filaments facilitate the engineering of prevascularised tissue engineering constructs.

1. Introduction

The advancement of cell cultivation techniques and biomaterial fabrication has largely contributed to the recent developments in engineering three-dimensional artificial tissues and organs. Significant steps towards complex functional biological tissues were achieved with the profound acceptance that a sufficient supply with oxygen and nutrients can improve the survival of the tissue construct. Prevascularisation strategies have emerged as a promising concept, aiming at avoiding hypoxic conditions and ensuring nutrient supply during the initial phase of cultivation. Furthermore, vascular structures strongly affect biological functions of parenchymal cells and microenvironmental cues. Particularly in the pharmaceutical field, the development of more predictive and physiological relevant in vitro tissues is an important goal to overcome the use of animal models.

Collagen has been widely studied for its application in tissue engineering, mainly as a scaffold forming a three-dimensional environment for cells or as a coating to accelerate cell adhesion to synthetic or natural biomaterials. Besides various favorable properties, collagen provides receptor–ligand binding sites for several cell types and thereby activates fundamental cellular processes including proliferation, migration and differentiation. Especially endothelial cells (ECs), the functional unit of a blood vessel, show significant responses in the presence of a collagen-based substrate. It has been shown that collagen I regulates endothelial cell adhesion, spreading and motility by recruiting RhoA to specific actin focal domains [1]. Furthermore, the adhesion of cell surface integrins to the ECM component in the presence of vascular endothelial growth factor (VEGF) activates the p44/p42 (Erk1/Erk2) mitogen-activated protein kinase (MAPK) signal transduction pathway and thereby regulates EC proliferation and survival [2]. It has long been recognized that triple-helical collagen I induces the formation of spindle-shaped morphology and capillary-like structures in EC cultures indicating a role in angiogenesis [3,4]. In contrast, fibroblast do not respond to collagen I with tubular structures, suggesting a specific role of collagen I in EC morphogenesis [5]. Therefore, collagen is a promising starting material for the fabrication of artificial blood vessels.

In recent years, several studies showed that ECs arranged within collagen tubes and hollow fibres recapitulate normal biological architecture. Oneoet al. [6] fabricated a thin but very long cell-containing microfibre called cell fiber. The hydrogel microfibre consisted of an inner core of ECM proteins covered with a mechanically more stable outer layer of calcium (Ca)-alginate and was generated using a double-coaxial laminar flow microfluidic device. ECs in fibres containing collagen I formed cell-cell-contacts and a tubular structure within 4 days of culture. The authors assembled the cell fibres into 3D macroscopic cellular constructs including tubular structures with a diameter of 1 mm and approximately 10 mm length using a glass rod. Finally, the Ca-alginate shell was enzymatically digested to achieve cell-cell contacts between neighboring fibres. Similarly, Goa et al. [7] applied a coaxial printing technique to generate small diameter tissue engineered blood vessels using a mixture of a collagen-rich ECM hydrogel and Ca-alginate. The engineered blood vessel contained endothelial and muscular cell layers. Resistance to blood pressure has been demonstrated in vivo in a rat model. However, measurements in both studies indicated low mechanical stability, although Goa et al. improved mechanical strength compared to an earlier study [8].

* Corresponding author.
E-mail address: ina.prade@filkfreiberg.de (I. Prade).

https://doi.org/10.1016/j.bbiosy.2022.100067
Received 30 December 2021; Received in revised form 8 October 2022; Accepted 9 October 2022

The direct fabrication of vascular structures using collagen I hydrogels is difficult because gelation is slow and must be strictly controlled in terms of temperature und pH value. To improve shape fidelity and mechanical strength researchers have used chemically modified collagen including photo-cross-linkable collagen [9,10], increased collagen concentrations [10,11] or rapid pH changes [12] to accelerate collagen self-assembly. However, the direct fabrication of freestanding tubular structures made of collagen has not yet been successful. In this study, we present (i) self-standing, (ii) long time storable and (iii) easy-to-use collagen hollow filaments that support the growth of endothelial cells in three-dimensional conditions. A collagen fiber suspension of minced decellularized porcine tissue was used to fabricate these filaments. During the manufacturing process, neither Ca-alginate or a similar support material nor sacrificial templates are involved, resulting in a direct and straightforward generation of hollow filaments. Human ECs were cultivated in the lumen of the collagen tubes for a period of 14 days under static and perfused conditions. Cell viability, marker expression and cellular response to continuous pulsatile flow was analyzed more in detail to determine if the collagen filaments were suitable for application in vascular tissue engineering.

2. Materials and methods

2.1. Collagen material

The collagen material was obtained from porcine hides. The raw material was washed and decellularized. Decellularisation was performed using a sodium sulfide liming process [13,14], followed by a second liming process using 3% lime for 3 days at 28 °C, deliming with ammonium chloride [13] and an incubation with 8% sodium bicarbonate for 6 h. The material was then disinfected with 10% hydrogen peroxide, washed intensively with water and pre-ground in a meat grinder. A stepwise dilution with water led to a liquid suspension, which was adjusted to pH 2.8 with hydrochloric acid and further comminuted with a colloid mill (IKA, Magic Plant). The collagen suspension was neutralized with sodium hydroxide solution and stored at −20 °C for at least 48 h. The efficient removal of antigenic components from the collagen material by the decellularisation process was shown in immunofluorescence stainings for DAPI (absence of nuclei) and galactose-alpha-1,3-galactose (α-Gal) and double checked by determining the total sugar content (see Supplements).

After thawing, the collagen material was separated from water using a sieve. The resulting agglomerate was dialyzed with Aqua bidest and adjusted to a dry substance content of 4.5% (w/w) and a pH value of 3.5 by adding Aqua bidest and hydrochloric acid (HCl).

2.2. Fabrication of collagen hollow filaments

Hollow tubes were fabricated by extruding a collagen suspension (dry substance 4.5%) through a core-shell nozzle with a diameter of 1.2 mm (diameter inner core: 0.5 mm) using the 3D printer bioscaffolder 3.2 (Gesim, Radeberg, Germany). The freshly extruding hollow filament was directed into a precipitation and cross-linking bath containing 70% ethanol in ultrapure water and 2% (w/v) 1-Ethyl-3-(3-dimethylaminopropyl)carbodiimide (EDC). After an incubation time of 30 min at RT the filaments were washed three times for 20 min in ultrapure water and manually wrapped around petri dishes. Finally, wet fibres were frozen and freeze-dried overnight.

2.3. Scanning electron microscope (SEM) analyses

Dry collagen hollow filaments were mounted onto specimen holders and sputtered with a thin layer of gold. Photos were taken by the SEM system (FEI Quanta 250 FEG) at an accelerating voltage of 10 kV.

2.4. Oxygen permeability

Oxygen diffusion was measured using oxygen-depleted water. Therefore, oxygen was removed from 1000 ml Aqua dest by infusing gaseous nitrogen for 30 min. The diffusion of oxygen through the tube wall was measured similarly to protein permeability. Collagen membranes were fixed in the two-chamber system and the chambers were filled simultaneously with Aqua dest or oxygen-depleted water. Immediately after complete filling, an oxygen sensor (PreSens Precision Sensing GmbH) was inserted in the low-oxygen fluid and the oxygen content was measured every 30 s for up to 5 h. The mean values for each group (cross-linked versus non-cross-linked, $n = 3$) shown in the diagram represent three independent measurements.

2.5. Protein permeability

Permeability of the collagen filaments for proteins was investigated using a self-made experimental setup (Fig. 2A). The system is intended for experiments with planar materials. It consists of two transparent chambers that can be separated with a foil or a membrane. A small inlet on the upper site of both chambers enables the injection of test solutions or the collection of test samples using a needle. To emulate the wall of the hollow filaments, the collagen material was used to prepare membranes with a similar thickness. The membranes were fabricated analogous to the hollow filaments. In brief, collagen suspension was poured into petri dishes, dried at RT and cross-linked with 2% EDC in 70% ethanol for 30 min at RT. Freeze-dried collagen membranes were fixed between the chambers. Both chambers were filled simultaneously with DMEM and 10% FBS on one side and Aqua dest on the other side. In both chambers 4% penicillin/streptomycin was added to counter potential contaminations. The liquids in the chambers were stirred during the experiments. At defined time points, three times 300 µl samples were taken from the target chamber (= protein-free chamber). The samples were stored frozen until further use. At the end of the experiments the protein content in the samples was analyzed with the Pierce BCA protein assay kit (Thermo Scientific). The amount of proteins in µg/ml was calculated from a standard curve. This curve was generated by serial dilution of FBS in Aqua dest. Three independent experiments were performed. One representative experiment is shown. For each group (cross-linked versus non-cross-linked) the mean values per time point from three samples were statistically analyzed.

2.6. Dextran permeability

The collagen hollow filaments were rehydrated in PBS for 30 min. Both channel openings were threaded onto 23 G needles, inserted in a perfusion chip (self-made, Fig. 2E) and connected to a perfusion system consisting of tubing and a piezo pump (Bartels, mp6 lowdriver). Inside the perfusion chip, the hollow filament passed through a rectangular chamber filled with 6 ml PBS. The hollow filaments were perfused with PBS for 2 min at a flow rate of about 400 µl/min. Then the PBS in the tubing was replaced with PBS containing 0.1 mg/ml Dextran Texas Red 70,000 MW. At a specific time point, 3 × 100 µl liquid samples were taken from the chamber, transferred to a black 96-well plate and analyzed in a multimode plate reader (Molecular Devices, SpectraMax i3x) (excitation 583 nm, emission 610 nm). Sampling was repeated at defined time points as long as the filament was completely covered with the liquid in the chamber. Four hollow filaments per experiment were analyzed.

2.7. Swelling behavior

Dry hollow filaments were cut into 750 µm thin slices with a cutting tool that consisted of several razor blades fixed at a defined distance on a metal rod. The slices were placed under a stereomicroscope (Zeiss,

Discovery.V12). Swelling of the material was monitored at 37-fold magnification after addition of PBS. The maximum degree of swelling was reached after 15 min. The outer and inner diameter of the tubes and wall thickness were calculated in microscopic images using ZEN core v2.7 software. Three sections per filament were analyzed. Three independently fabricated hollow filament batches were measured. From each batch, three filaments were used.

2.8. Enzymatic degradation

Stability of collagen hollow filaments against enzymatic degradation was analyzed using Collagenase from *Clostridium histolyticum* (type IA). Non-crosslinked filaments were used as controls. The extrusion of the (non-crosslinked) control fibres was done without adding crosslinker to the precipitation bath during filament production.

Collagen tubes were weighed and rehydrated in 0.2 M ammonium carbonate buffer (pH 7.5). Then, 0.05 M calcium chloride, penicillin/streptomycin (1:100) and collagenase in a final amount of 0.06 CDU (collagen digestion units) per mg (related to the dry mass of collagen) were added. Samples were incubated for 7 days at 37 °C in a thermal shaker at 750 rpm. The digestion was stopped using a protease inhibitor cocktail (Sigma-Aldrich). Samples were centrifuged for 5 min at 14,000 rpm, supernatant was discarded and the pellet was washed three times with Aqua bidest. The undigested residue was dried in a drying cabinet at 30 °C and finally weighed again. The degree of degradation was calculated as follows: degradation [%] = 100 x dry weight after digestion / dry weight before digestion. Three samples per time point were analyzed.

2.9. Mechanical testing

Uniaxial tensile testing was performed using a Zwick universal testing machine (ZwickRoell Z0.5) and a force transducer of 100 N. Collagen hollow filaments were manually loaded until reaching positive tension and tensile loads were applied to the fibres at a 5 mm/min loading rate until breakage. Tensile stress and strain as well as ultimate tensile strain were recorded. Young's modulus was calculated based on the slope of the stress/strain curve. Samples were tested in dry state and after 30 min rehydration in PBS. In each group (dry, rehydrated) five samples were measured.

2.10. Cell cultivation

Human umbilical vein endothelial cells (HUVECs; Lonza) were cultured in EGM-2 (EBM-2 supplemented with Single Quots; Lonza) and grown as monolayer cultures in T75 flasks (Greiner Bio-One, coated with Speed coating from PeloBiotech). Cells were incubated at 37 °C in an atmosphere containing 5% of CO_2 and with a relative humidity of 95%. Accutase (Sigma-Aldrich) was used to subculture the cells twice a week. The cell number was determined with a Neubauer counting chamber (Paul Marienfeld).

2.11. Collagen hollow filament colonization

Prior to cell seeding, 10–20 mm long hollow filaments were rehydrated in EGM-2 for at least 15 min at RT. At least 2.5×10^5 cells in 150 µl EGM-2 were injected into a filament using a 25 G needle (outer diameter 0.51 mm). The cell suspension was injected from one side. Suspension that ran out was reinjected from the other side. Hollow filaments were kept for 20 min at 37 °C in the incubator to allow cell adhesion. No additional medium was added and the well plates with the tubes were flipped every 5 min. During this procedure, tubes stuck to the bottom of the well. Cell-laden filaments were transferred into a new 6-well plate, supplied with fresh culture medium and incubated in the CO_2-incubator.

Reproducibility of cell colonization was analyzed separately using a phosphatase assay. Cell-laden collagen tubes were lysed with lysis buffer and incubated with phosphatase substrate (Sigma-Aldrich). After 30 min at RT, the cell-laden tubes were cut longitudinally and transversely and incubated further for 60 min at RT. Reaction was stopped with 2 M sodium hydroxide solution and 2×100 µl of the yellow supernatant was transferred to a 96-well plate and analyzed in a plate reader (Molecular Devices, SpectraMax i3x) at 405 nm. The resulting OD values were averaged and set to 100%. The standard deviation of all values represents the difference in seeding efficacy and is shown in%. Reproducibility of cell colonization was analyzed in three independent experiments. The result of one representative experiment ($n = 6$) is shown in the text.

2.12. Cultivation of cell-laden hollow filaments

One day after cell seeding, a 6-well plate with cell-laden filaments was taken from the incubator. A sample of a few millimetres was cut from one or two randomly selected filaments, stained with Calcein AM and propidium iodide and analyzed microscopically (according to Materials and methods: cell viability). When the cells in the filament samples were nearly confluent, the vascular structures in the incubator were perfused using an external pump system. In case cells showed low cell density in the samples, all cell-laden collagen tubes were incubated with EGM-2 media in a 6-well plate without perfusion (static culture) until cells number increased significantly. For the perfusion, cell-laden tubes were thread onto a 25 G needle without additional fixation. The needles were inserted for at least 3 mm and a maximum of 4 mm. The filament-needle construct was placed in a modified 6-well perfusion plate (Alvetex perfusion plate, Reprocell Europe Ltd.) and connected to a technical perfusion system using a luer lock adapter. Vascular constructs were perfused with a continuous pulsatile medium flow using the PDMS free modular plug and play construction kit from Fraunhofer IWS [15]. This perfusion setup consists of flexible tubing and triple pump chips driven by an MPS (microphysiological systems) control system. The triple pump chips contain pneumatically driven peristaltic micro pumps that generate a pulsatile volume flow. Medium flow was set to 110 μl/min and vascular constructs were cultivated for up to 14 days. Static control cells were cultured in 6-well plates. Culture medium was changed every 2–3 days.

2.13. Calculation of shear stress

The shear stress in the perfused collagen hollow filaments was calculated using the Elveflow's online microfluidic calculator [16]. To avoid cell damage, a low pump rate was chosen. The volume that was perfused in a given time was measured and revealed a flow rate of 110 µl per minute. The rate was chosen randomly. The following parameters were used for the calculation of the shear stress: lumen diameter 790 µm, length 20 mm, viscosity EGM-2-medium $\mu = 0.78$ cP [17].

2.14. Cell viability

Cell viability was analyzed after a cultivation period of 3, 7 or 14 days. Cell-laden tubes were transferred into a 6-well plate and stained using 0.5 µl Calcein AM/ml (Sigma-Aldrich) and 2.2 µl propidium iodide/ml (PI, Sigma-Aldrich) for 30 min at 37 °C. Then, the medium was exchanged and cells were viewed with a confocal laser microscope (Zeiss, LSM800) with 488 nm (green, Calcein AM) and 561 nm (red, PI) excitation filters. Fluorescence signals were detected through the filament wall without cutting the tubes. Images were captured at 200-fold magnification. Six samples from every group (static, perfused) at each time point were analyzed and three images per sample were acquired. Images were analyzed using ImageJ software and live and dead cells were counted using the multi-point tool. Viability was calculated as percentage of living cells.

2.15. Analyses of shrinkage of collagen hollow filament

Shrinkage of the collagen filaments during cultivation was analyzed with pieces of 10 mm length. Individual cell-laden and cell-free collagen tubes were transferred into 6-wells and fully covered with EGM-2 media. Medium was changed every 2–3 days. After 7 and 14 days of incubation at 37 °C in a CO_2-incubator, collagen tubes were analyzed with a stereomicroscope (Zeiss, Discovery.V12) and Zeiss software (ZEN core v2.7). Three independently fabricated collagen filament batches were tested. From each batch three filaments were analyzed in triplicates.

2.16. Detection of ve cadherin in cell-laden hollow filaments

Cell-laden hollow filaments were fixed with ice-cold methanol for 10 min at −20 °C. The constructs were halved lengthwise with a razor blade, washed three times for 5 min with washing buffer (0.5% Tween 20 in PBS*) and blocked with 3% goat serum (Jackson ImmunoResearch Europe Ltd) in washing buffer for 30 min. Rabbit anti-VE cadherin antibody (Cell Signaling Technologies, catalog #2500S) was diluted 1:100 in blocking buffer (3% normal goat serum in washing buffer) and incubated on the samples overnight at 4 °C. The constructs were washed three times for 5 min with washing buffer and goat-anti rabbit IgG-FITC (Santa Cruz, 1:200 in washing buffer) was added for 1 h at RT. Finally, samples were washed again three times for 5 min in washing buffer, stained with DAPI (Thermo Fisher Scientific, 1:1000 in washing buffer) and analyzed after another washing step using a cLSM (Zeiss, LSM800; magnification 400-fold).

2.17. Endothelial cell orientation

Flow-induced orientation of cells was measured with cells cultivated for one or two days under static and perfused conditions. HUVECs were exposed to shear stress of either 0.3 or 0.9 dyn/cm^2. Cell orientation angle was measured in fluorescence images of cells stained with VE-cadherin (Cell Signaling Technologies, catalog #2500S) and DAPI (Sigma-Aldrich). The longest axis of each cell was manually markered using the straight line tool of ImageJ software. ImageJ calculated the orientation angle of each cell. The measured angle is the angle between the cell axis and a line parallel to the x-axis of the image (90° represented the direction of flow). At least 5 images per sample were measured. Three samples per group (static, perfused) were analyzed. Orientation angles were categorized in classes of 10° The angle value for each cell was used to plot the histograms in Fig. 5. Additionally, the mean orientation angle from each group (static versus perfused) was calculated. Orientation was anlayzed in three independent experiments. The data in Fig. 5 show the results of a representative experiment.

2.18. Synthesis of extracellular matrix components

The expression of extracellular matrix proteins including laminin, fibronectin and collagen type IV was detected in immunofluorescence images. For the detection of laminin and fibronection: cells grown in perfused hollow filaments for 14 days were fixed with 3% PFA for 20 min at RT. Then, cells were first incubated with 0.25% Tween 20 in PBS* for 10 min at RT and then washed with 0.2% Triton X-100 in PBS*. Fixed hollow fibres were treated with 4 mg/ml pepsin (Serva, porcine, catalog #31,820, 15 mAU/mg) in 0.01 M HCl for 10 min at 37 °C to expose the ECM molecule's epitopes according to Antons et al. [18] and then blocked with 1% goat serum in PBS* for 30 min at RT. Collagen type IV was analyzed after fixation of the cells with ice-cold methanol for 10 min at −20 °C. Fixed cell-laden hollow fibres were halved lengthwise with a razor blade, washed three times for 5 min with washing buffer (0.5% Tween 20 in PBS*) and blocked with 3% goat serum (Jackson ImmunoResearch Europe Ltd) in washing buffer for 30 min. Proteins were labelled with the following primary antibodies: anti-fibronectin (BD Bioscience Transduction Laboratories, catalog #610,077, 1:50) and anti-laminin (Sigma-Aldrich, catalog #L9393, 1:50) and collagen type IV (Biozol, catalog #LS-C382816, 1:200) in blocking buffer. After incubation overnight at 4 °C, secondary antibodies were added in a dilution of 1:100 in blocking buffer for 1 h at RT: goat-anti-mouse IgG-FITC (Santa Cruz) for detection of fibronectin and goat-anti-rabbit IgG (whole molecule)-FITC (Sigma-Aldrich) for detection of laminin and collagen type IV. Finally, samples were washed three times for 5 min in washing buffer, stained with DAPI (Thermo Fisher Scientific, 1:1000 in washing buffer) and analyzed after another washing step using a cLSM (Zeiss, LSM800; magnification 400-fold).

2.19. Statistics

Statistical analyses were performed using JASP software (version 0.16). Mean values of the replicates were used to perform an independent *t*-test or an analysis of variance in case of more than two variables or groups (ANOVA, followed by a Tukey test and post hoc test according to Bonferroni-Holm). P-values of 0.05 were considered to be significant different. Details of the statistical tests used for each experiment can be found in the figure legends. Data are presented as mean values with standard deviation.

3. Results

3.1. Characterisation of the collagen suspension

This study uses collagen from porcine skin as a basic material to generate cell-laden vascular constructs. Although the clinical use of decellularized animal-based tissues is well established, antigen-mediated hyperacute reactions are still a critical issue. To control the quality of the decellularised collagen material, several analyses were performed. Mass spectrometry showed a high collagen type I content of 93% (Supplementary Figure 1). The collagen suspension had an ash content < 0.05% and a total nitrogen content of 17.4% (Supplementary Table 2). Analyzes of collagen fiber size revealed that most of the fibres were >1000 µm (Supplementary Table 2). The elimination of the major xenoantigen α-Gal (Galα1,3-galβ1–4GlcNAc-R) epitope was determined in immunofluorescence staining. No clear α-Gal signal was found in freeze-dried collagen material, indicating that the antigen was sufficiently removed during decellularisation (Supplementary Figure 2). Additionally, the total content of Galactose and Glucose was measured. Very low amount of monosaccharides remained in the collagen suspension (Galactose: 0.5 mg per g; Glucose: 0.05 mg per g dry substance) (Supplementary Table 3).

3.2. Fabrication and characterization of the hollow filaments

Porcine collagen suspension (Fig. 1A) was extruded through a core-shell nozzle of a 3D printer. Directly after leaving the nozzle, the extruded filaments were inserted into a cross-linking bath (Fig. 1B and D). Freeze-dried collagen filaments were semi-transparent (Fig. 1E) and relatively stiff. Rehydrated filaments were flexible and easy to handle with forceps (Fig. 1C and G). Scanning electron microscope (SEM) analyses revealed a smooth inner surface without pores (Fig. 1F and H, Supplementary Figure 3).

3.3. Oxygen and protein permeability

The main function of the vascular system is to supply oxygen and nutrients to the tissue. Therefore, the permeability of the vessel wall is essential. The hollow filaments should also feature this permeability to function in a similar way. Although a thin and partly porous filament wall was observed, the cross-linking and the closed inner and outer surface could probably hinder a sufficient penetration of oxygen and proteins. In order to characterize the suitability of the hollow fibres for their use as artificial blood vessel structures, permeability tests were performed. Oxygen diffusion through the collagen material was measured

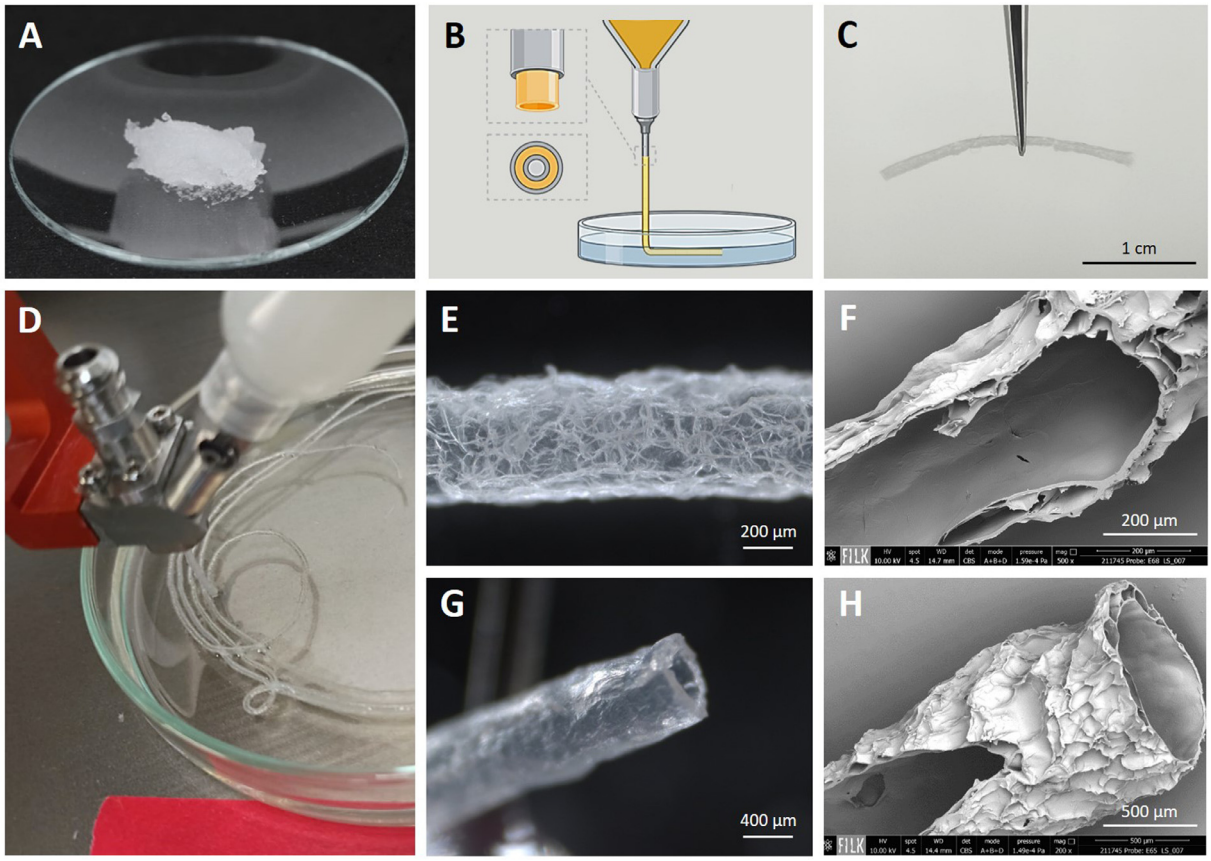

Fig. 1. Fabrication and appearance of collagen hollow filaments. A) Photograph of the collagen suspension shortly before use. B) Schematic drawing of the extrusion process in which hollow filaments are produced. **C)** Photograph of a wet hollow fiber handled with forceps. Scale bar = 1 cm. **D)** Photograph of the fabrication process using the core-shell system of the bioscaffolder printer. **E)** Stereomicroscopic image of a dry hollow tube. Scale bar = 200 µm. **F and H)** Scanning electron microscope images of hollow filaments. Scale bar = 200 µm (F) and 500 µm (H). **G)** Stereomicroscopic image of a wet, fully rehydrated collagen hollow filament. Scale bar = 400 µm.

with the help of a two-chamber system as shown in Fig. 2. Here, two cylinders were separated using a collagen membrane with properties similar to those of the hollow filaments (cross-linking degree, thermal stability, Supplements Table 4). It should be noted that the thickness of the membranes was about 4-fold higher compared to the filament wall to allow the fixation of the membranes between the cylinders without rupturing. An oxygen sensor was placed in the oxygen-depleted medium to monitor changes in oxygen content over a period of 5 h. Oxygen concentration increased by 5.2 ± 0.5% after 5 h compared to the starting point (Fig. 2B). Maximum oxygen content in the 'oxygen chamber' was 18%.

Protein permeability was also analyzed using the two-chamber system. Protein concentration increased constantly over time (Fig. 2C). Proteins of a wide range of molecular weights could pass the membrane (Supplementary Figure 4). These observations indicated that the collagen hollow filament is permeable for proteins. To confirm this, permeability tests were conducted with the hollow filaments. Dextran Texas Red with a molecular weight of 70,000 was perfused through the collagen filaments. Dextran permeability was analyzed in the liquid covering the filaments. A strong increase in fluorescence signal was measured within one hour (Fig. 2D).

3.4. Properties of the collagen hollow filaments

To assess the physical properties of the collagen tubes, the swelling behavior was determined. Furthermore uni-axial tensile tests were performed. In contact with PBS or cell culture medium the dry fiber rehydrates within 15 min resulting in a very flexible hollow filament with a wall thickness of 163.8 ± 22.8 µm and an inner diameter of 790.5 ± 65.2 µm (Fig. 3A, Supplementary Table 5). Collagen filaments were cross-linked to ensure long-time stability during cell cultivation. Incubation with collagenase enzyme showed that the resistance to enzymatic degradation was improved after cross-linking compared to non-cross-linked filaments (Fig. 3D). The filaments exhibit significantly different mechanical stability in dry and wet state, as expected. Dry collagen tubes appeared stiffer and had a higher ultimate tensile strength (UTS) of 10.9 ± 2.2 MPa (Fig. 3E) and maximum force of break (1.32 ± 0.4 N, Supplementary Table 5). The fibres elongated up to 4.1% under mechanical stress (Supplementary Table 5). Rehydrated fibres showed a slight increase in strain (5.4%) and a thirty-fold lower tensile strength of 0.34 ± 0.1 MPa. Young's modulus of wet fibres was also highly reduced (2.5 MPa wet vs. 21.2 MPa dry) (Fig. 3F).

3.5. Cell seeding and cell cultivation within the collagen filaments

The results showed that the collagen hollow filaments were stable in wet environment and possessed wall permeability for oxygen and proteins. These properties indicate that the tubes are good candidates for vascular tissue engineering approaches. Therefore, cell culture experiments with HUVECs were performed to investigate cellular viability of endothelial cells seeded within the hollow fibres. The percentage of living cells present in the filament after seeding varied (100 ± 18.3%, no diagram shown). However, live/dead staining revealed a high number of living cells in the hollow filaments. Green fluorescence of Calcein AM could be analyzed through the tube wall without sectioning (Fig. 3G - I).

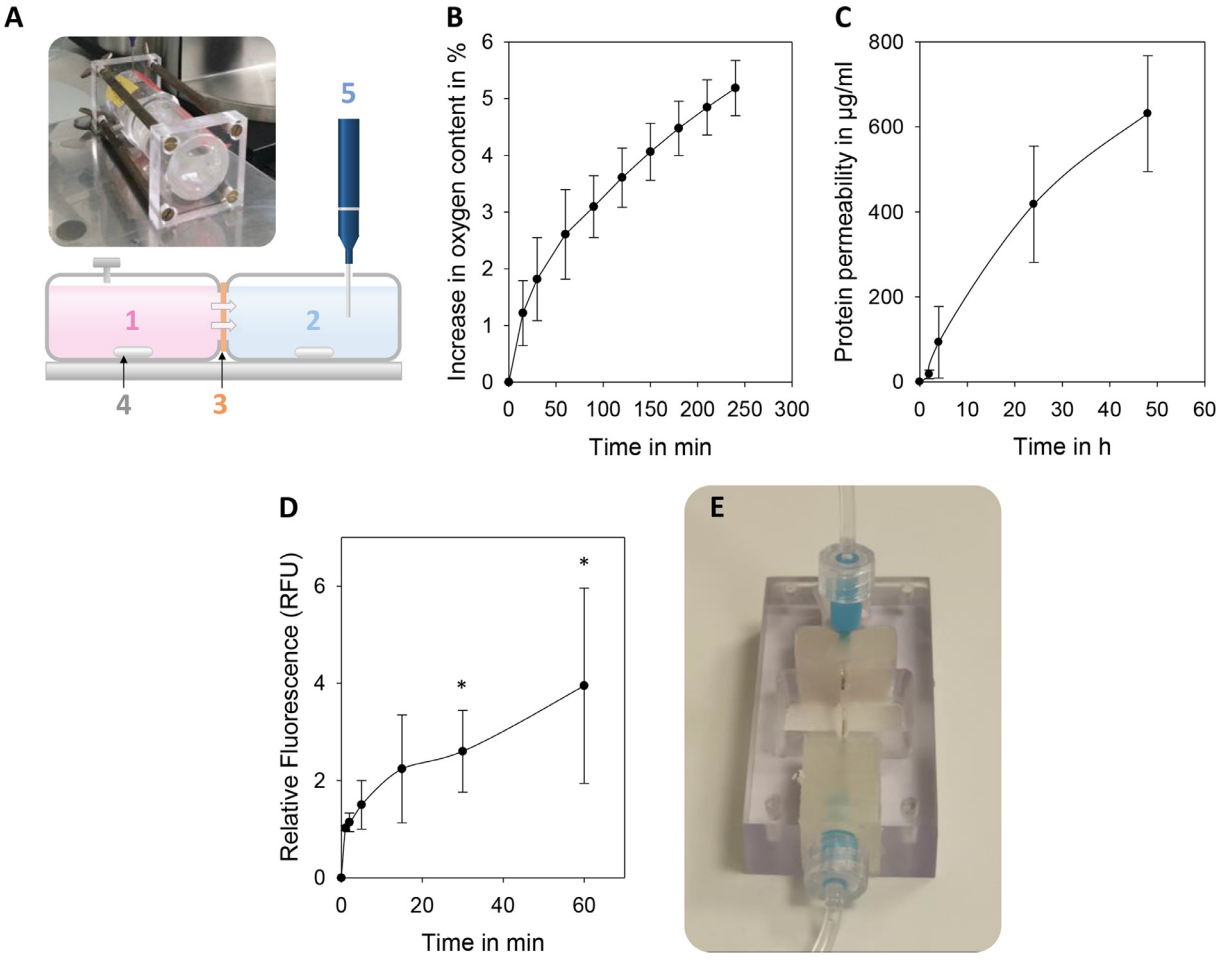

Fig. 2. Permeability for oxygen and proteins. A) Schematic illustration and photograph of the experimental set-up for measuring the oxygen and protein permeability. 1 – nutrient/oxygen chamber, 2 – target chamber, 3 – collagen membrane, 4 – stirrer, 5 – oxygen sensor. **B)** Changes in oxygen concentration in the oxygen-depleted chamber over time. **C)** Amount of protein in the target chambers at different time points. **D)** Changes in relative fluorescence intensity over time in surrounding liquid during the perfusion of Dextran Texas Red 70,000 MW through the collagen hollow filaments. **E)** Photograph of the experimental set-up of the dextran permeability tests. The collagen hollow filament passed through a chamber filled with liquid. During perfusion of the dextran, fluorescence intensity was measured in fluid samples taken from the chamber.

The cells were cultured under static or perfused conditions. For the perfusion of cell culture medium through the hollow filaments, cell-laden collagen fibres were cannulated using a 25 G cannula (Fig. 4A and B). Flexible tubings were connected to the cannulas and medium was perfused with a volume of 110 µl per min. Cells were cultivated for 14 days. After 6 days at the earliest, HUVECs formed a confluent monolayer in perfused collagen filaments (Fig. 4C, F and G). The number of live and dead cells was determined at different time points. Under static conditions, the number of dead cells increased as cultivation time progressed and cell number rose (Fig. 4D and E). Perfusion of culture medium significantly improved cell viability in the tubes (Fig. 4D and E).

Collagen hydrogels tend to shrink during cell cultivation. This is particularly disadvantageous when the constructs are connected to an in- and outlet port as it is usually the case for vascular constructs. In this study, a collagen suspension was used for the fabrication of the filaments. The changes of the length and the outer diameter of the collagen hollow filaments was monitored over a cultivation time of 14 days. Only a slight shrinking was observed in length (8%) but not in width in the presence of HUVECs (Fig. 4H and I). The shrinkage of cell-laden hollow fibres was similar to filaments incubated in media without cells. Cross-sections revealed that HUVECs adhered to all sites within the hollow filament (Supplementary Figure 5) indicating that the cells applied forces over the whole perimeter. Comparable results were obtained with primary human smooth muscle cells (SMC). The change in the length of filaments seeded with SMCs was <12% (Supplementary Figure 6 A and B). SMCs showed a homogenous coverage of the outer surface of the filaments (Supplementary Figure 6 C – E).

Blood flow is an important regulator of endothelial cell physiology and vascular function. A healthy endothelium responds to fluid wall shear stress by remodeling the actin cytoskeleton resulting in changes in cell shape and orientation. To characterize the flow properties in the perfused collagen hollow filaments, the shear stress was calculated using the Elveflow's online microfluidic calculator. A value of 0.3 dyn/cm^2 indicated a very low shear rate. In addition, the Reynolds number revealed laminar flow. As endothelial cells elongate and align with a defined direction of flow, orientation of endothelial cells cultured in collagen hollow fibres was measured after at least two days under perfused conditions. Although the flow rate was very low, significant differences between static and perfused cultured cells were observed. Increasing the shear stress to 0.9 dyn/cm^2 revealed similar results. Under static conditions endothelial cells showed no specific orientation (Fig. 5A and D). The mean orientation angle was 45.9 ± 7 ° (Fig. 5C). Contrary, in the presence of media perfusion, cellular orientation changed towards

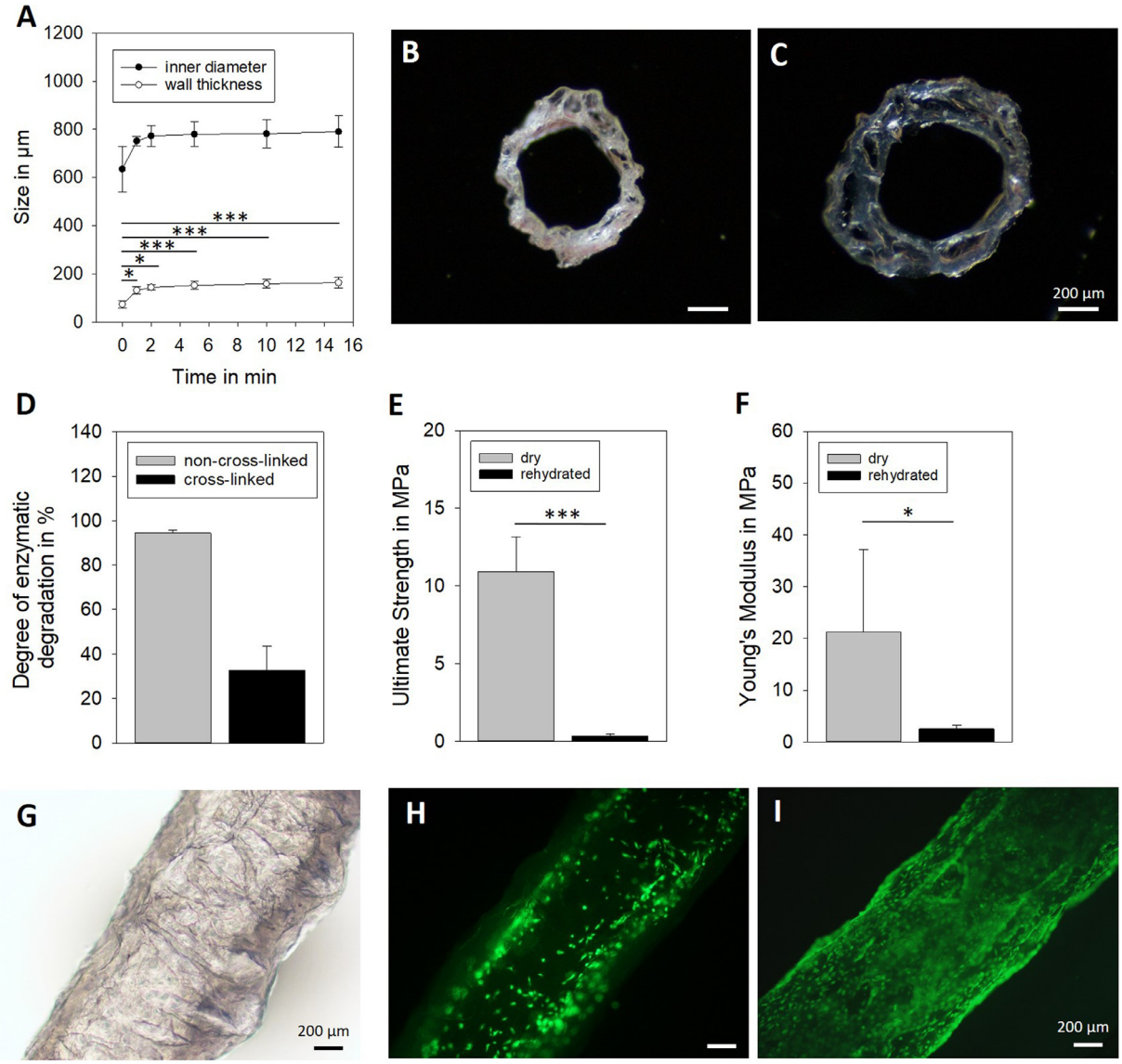

Fig. 3. Properties of collagen hollow filaments. A) Absolute values of the inner diameter and wall thickness of the collagen hollow fibres during rehydration with PBS. Student's *t*-test; $^{*}p < 0.05$; $^{***}p < 0.001$. **B and C)** Light microscopy images of the hollow tubes before (B) and after rehydration (C). Scale bar = 200 µm. **D)** Percentage of degraded collagen after enzymatic digestion with collagenase. **E and F)** Ultimate strength (E) and Young's Modulus (F) of collagen hollow tubes in uniaxial tensile tests. Gray = dry, black = fully rehydrated. Student's *t*-test; $^{*}p < 0.05$; $^{***}p < 0.001$; for E) the alternative hypothesis specifies that group dry is greater than group rehydrated. **G)** Light microscopy image of a cell-laden collagen hollow fiber. **H and I)** Calcein AM staining of cell-laden collagen hollow filaments one day (H) and 14 days (I) after seeding of HUVECs, non-perfused conditions. Scale bar = 200 µm.

the direction of flow and an orientation angle of single cells < 50° was less pronounced (Fig. 5A, C, E and F). Mechanical forces transmitted via the cytoskeleton also affect nuclear shape and structure. Media perfusion significantly reduced the nucleus area in HUVECs compared to static conditions (Supplementary Figure 7). These data indicate that the endothelium formed within the collagen fibres is able to respond to shear stress. Immunofluorescence staining of the cell-cell junction protein vascular-endothelial cadherin (VE-cadherin) was performed to identify cell orientation. It is well known to be an important component of endothelial mechanotransduction. VE-cadherin signal was detected at the cell borders in HUVECs grown under perfused (Fig. 5B, E and F) and static conditions (Fig. 5D). However, we also observed that the smooth inner surface was important for the formation of those cell-cell-contacts. Hollow filaments extruded into a bath of PBS rather than 70% ethanol had a rough and porous inner surface (Supplementary Figure 8 C and D). Cultivation of HUVECs in these filaments showed significantly less VE-cadherin positive cells (Supplementary Figure 8 E to K).

Remodeling of the underlying ECM is another important feature of ECs. Deposition of the ECM proteins collagen type IV (Fig. 5G), laminin and fibronectin (Supplementary Figure 9) was detected, indicating that the cells actively synthesized structural proteins of the basal membrane. Hence, ECs cultured in collagen hollow filaments showed typical characteristics of a healthy endothelium.

4. Discussion

The lack of mechanical stability is a bottleneck for development of engineered vascular constructs especially with materials that mainly consist of collagen. In this study, mechanically stable and cell-laden fibres are described that enable the fabrication of long vascular con-

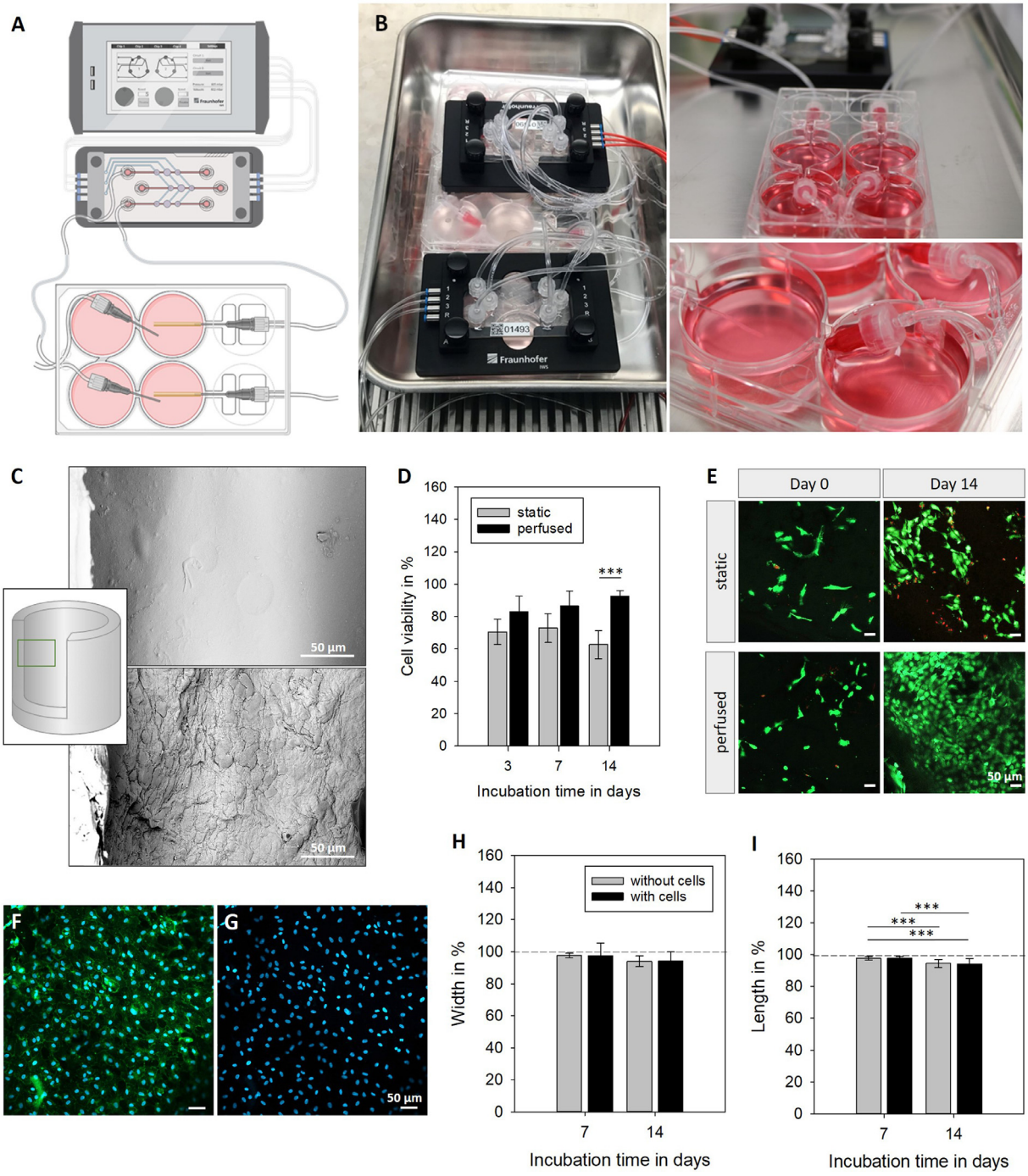

Fig. 4. Cell cultivation within the collagen hollow filaments. A) Schematic illustration of the experimental set-up for cell cultivation under perfused conditions. **B)** Photographs of the cultivation system that allowed hollow filament perfusion. **C)** Scanning electron microscope images of the inner surface of hollow filaments without (top) and with cells (bottom). The position of the microscopic images within the hollow filaments is shown in the schematic drawing (green square). Scale bar = 50 µm. Cells were cultured for 6 days (not constantly perfused). **D)** Cell viability of HUVECs cultured up to 14 days in the collagen tubes. Two-way ANOVA; *** $p < 0.001$. E) Live/dead staining of cell-laden collagen hollow fibres on day 0 and 14 of cultivation and under static or perfused conditions. Fibres are uncut. Scale bar = 50 µm. F and G) Confocal images of VE-cadherin staining and DAPI nuclear marker in HUVECs cultured on the surface of collagen hollow filaments for 6 days under non-constant perfusion. Scale bar 50 µm. **H and I)** Changes in the width and the length of collagen fibres in the presence or absence of HUVECs. Two-way ANOVA, *** $p < 0.001$.

structs. The collagen fibres are flexible in wet conditions and can be handled with common tools in the laboratory. During the extrusion printing process, neither supporting nor sacrificial materials are required, resulting in direct fabrication of collagen hollow tubes. These freestanding structures can serve as an easy-to-use component to provide individual sizable supply channels for the generation of three-dimensional artificial tissues.

Different strategies, including rolling of cell-sheets [19], hydrogel mold-casting [20,21] and 3D bioprinting [6,12,22] have been utilized to create collagen hollow channels that support endothelial growth. How-

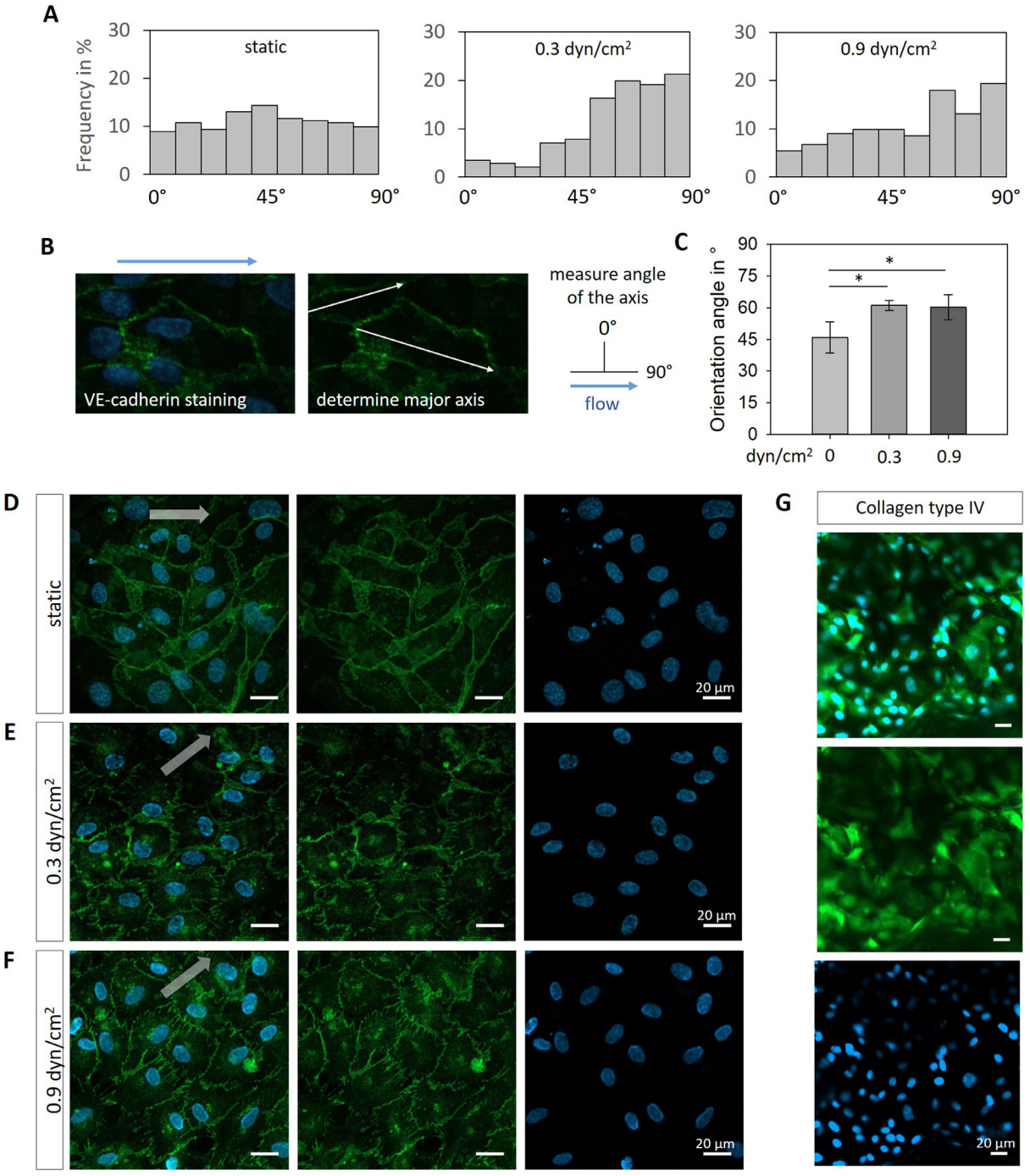

Fig. 5. Analyses of the endothelial layer. A to C) Cell orientation in perfused collagen hollow filaments**. A)** Quantification of cell orientation angle (direction of flow = 90°). Data represent frequency of cells per class (with 9 classes, each 10°; between 0° and 90°; $n = 3$). Static culture (left) and perfused culture (middle: 0.3 dyn/cm^2, right: 0.9 dyn/cm^2). **B)** Process of cell orientation measurement using cells stained with VE-cadherin. Orientation angle was calculated from the major axis of each cell. The axis was manually marked with a straight line and orientation angle was calculated in ImageJ. Right scheme illustrates the flow direction and corresponding cell orientation angle. **C)** Quantification of mean cell orientation angle of HUVECs grown within the collagen filament channel for two days under static and perfused conditions. Student's *t*-test; $^*p < 0.05$, calculated for the hypothesis that perfused cells show a higher mean angle than non-perfused cells. **D to F)** Confocal images of VE-cadherin staining and DAPI nuclear marker in HUVECs cultured for 3 days under static (D) or perfused conditions (E and F) in the collagen hollow filaments. Arrows indicated the direction of flow. Scale bar = 20 µm. **G)** Confocal images of collagen type IV staining and DAPI nuclear marker in HUVECs cultured for 14 days in perfused collagen hollow fibres. Scale bar = 20 µm.

ever, these studies resulted in fragile tissue engineered constructs that are often limited to a few millimeters. During the fabrication process, mandrels are often necessary to shape collagen material [23,24,25]. After removal of the solid core, tube diameters between 1 and 4.75 mm are described in the literature. In the study here, much thinner hollow collagen filaments were fabricated with an outer diameter of < 800 µm and a wall thickness of < 80 µm (dry) using a simple and cost effective extrusion printing process. Several groups showed the successful fabrication of collagen fibres and microfibres with extraordinary mechanical properties [26–28]. However, studies describing mechanically

stable hollow fibres for cell culture applications are still rare. Zhang et al. [29] reported on the coaxial printing of perfusable sodium alginate hollow fibres. Dehydrated fibres had a diameter of 788 μm. Rehydration of alginate fibres lead to full swelling after 4 h. The manufactured collagen tubes in our study achieved full rehydration after 15 min. Moreover, collagen hollow filaments showed a thinner tube wall than the alginate tubes (164 μm vs. ~200 μm), but their Young's Modulus and maximum strain were at least 3- and 7-fold higher, respectively. Shen et al. [30] generated collagen hollow fibres under coaxial flow using a microfluidic device. The collagen solution was continuously injected into a microfluidic channel together with a second preparation (Ca-alginate or medium) that formed the core of the fibres. The resulting core-shell structure was immersed in a gelation solution and cross-linked for 3 h using EDC. The resulting hollow tubes with an outer diameter of 500 μm and a wall thickness of 200 μm only reached a Young's Modulus of 0.24 MPa (with alginate core). Triple-coaxial bioprinting of bilayer small-diameter tubes made of ECM components and alginate showed an increase in ultimate tensile strength after two weeks cultivation with perfusion in a bioreactor [7]. Still, ultimate tensile strength was lower compared to UTS of collagen hollow filaments (0.2 MPa versus 0.34 MPa). Additionally, the authors reported a severe shrinkage of the vessel construct with drastical drop within the first days of culture. Wall thickness was reduced by 46% compared to the initial values after fabrication. The length of the vessels showed changes of about 18% [7]. Collagen hollow fibres of this study shrank by only 8% in diameter in the presence of ECs. It has been shown that primary smooth muscle cells cause stronger contraction of collagen hydrogels compared to primary endothelial cells [31]. Therefore, the shrinkage of collagen filaments in the presence of SMCs was additionally analysed. Similar to the endothelial cells, the filaments shrank only slightly, indicating a dense packing of collagen during fabrication of the tubes. In contrast to collagen hydrogels, the filaments are prepared from a collagen suspension, which contains natural grown collagen fibres [32]. These hierarchical structures consist of highly ordered fibrils and intermolecular cross-links providing higher resistance to multidirectional mechanical loading compared to single collagen molecules and individual fibrils [33–35]. Additional cross-linking of the fibres using EDC directly after printing may have further accelerated mechanical stability. Thus, hollow filaments made of collagen suspension have improved mechanical properties that allow for easy handling and long-term perfusion.

Sufficient oxygen transport is required for adequate cellular function and viability of a tissue-engineered construct [36]. Magliaro et al. [37] measured the decrease in oxygen concentration in a closed cell culture chamber containing a 3D hepatocytes culture in a collagen hydrogel. The authors observed that the cells consume the majority of the oxygen within the first hour of cultivation. Oxygen permeability tests in our study revealed sufficient oxygen diffusion through the collagen material. The oxygen content increased by 5% within 2 h (refers to a maximum oxygen content in a humidified incubator = 18.6% [38]). The tests were performed using a collagen membrane with a thickness of 750 μm. The wall of a collagen filament has a thickness of 164 μm. Cross-linking as well as an increase in collagen membrane thickness and density have been shown to lower the diffusion coefficient [39,40] suggesting a much faster diffusion of oxygen through the filament wall. This finding confirms the permeability of the collagen filaments to oxygen. Permeability tests with fetal calf serum or fluorescence-labelled dextran (70,000 MW) revealed that proteins with a high molecular weight are also able to pass the collagen material. The data suggest that collagen filaments could potentially be used to deliver growth factors or pharmaceutical substances into an artificial tissue construct. Instead of tubes made of synthetic polymers, cell-laden collagen filaments offer a more physiologically relevant vascular structure for drug testing or the realization of pathological in vitro models.

ECs showed good cell adhesion and spreading on the inner wall and distributed over the whole perimeter of the collagen hollow fibres. It can be assumed that the smooth inner surface of the filaments supported the uniform coverage with ECs and has contributed to the very high cell viability observed under perfusion conditions. The smooth surface was probably caused by the addition of 70% ethanol to the cross-linking bath. Bak et al. [41] investigated the effect of ethanol-based dehydration for the fabrication of collagen microfibers. The authors observed a smooth and highly uniform surface of microfibres after incubation with 70% ethanol. This is induced by a rapid precipitation of the collagen material due to the removal of loosely bound water. Fibres dehydrated with ethanol ≤ 50% or ≥ 90% showed a rough surface [41]. The extrusion of the collagen suspension into a bath without ethanol in the study here confirmed this observation. Collagen hollow filaments showed a rough and porous inner surface. HUVECs seeded in those filaments showed a much lower number of VE-cadherin positive cells compared to HUVECs grown in the smooth collagen filaments.

Endothelial cells form a semi-selective barrier between the bloodstream and surrounding tissues in vivo. This barrier controls the exchange of proteins, dissolved components and liquid, as well as the migration of cells including immune cells. VE-cadherin is an important regulator of these processes [42]. Additionally, it plays a major role in mechanotransduction enabling ECs to sense and adapt to shear stress [43,44]. A weakened barrier function and a loss of mechanical sensing is associated with pathological anomalies in vivo such as chronic inflammation, cardiovascular diseases and immune disorders [45]. Locally, endothelium dysfunction can lead to atherosclerotic lesions and disturbance in flow. In vitro studies show that such an environment promotes proinflammatory gene and protein expression in ECs [46] contributing to an increased susceptibility to a loss of barrier function and endothelial stability [47]. Confocal analyses showed that HUVECs formed tight cell-cell contacts with VE-cadherin being present at the cell borders. Additionally, the cells were able to express ECM proteins typically found in the basal membrane. Thus, immunofluorescence analyses revealed a well-formed endothelium at day 14 of culture. Cellular response to flow is another indicator for a functional endothelium. HUVECs cultured under media flow experienced low shear stress with a magnitude of < 1 dyne/cm^2. Alignment of endothelial cells to the direction of flow is usually observed with shear stress around 10 dyne/cm^2 [48,49]. However, morphological changes of ECs in rectangular channels were measured already at lower shear stress such as ≤ 3 dyne/cm^2 [50,51]. In our study, HUVECs are growing within a circular channel. A previous study from Bosch-Rué et al. [52] showed that cells behave differently when seeded in circular channels. The majority of cells aligned perpendicular to the longitudinal axis of the filament over time in the absence of shear stress. Although we could not observe this effect, substrate curvature plays obviously an important role in cellular orientation. If cells are more sensitive to flow when growing on a curved substrate is unknown so far. However, substrate curvature has recently been recognized as a critical cue for EC behavior [53]. In our study, HUVECs reorganized with very low shear stress indicating a higher sensitivity towards media flow and the ability to adapt to environmental signals within the hollow fibres. To our knowledge, no other study has been able to demonstrate these changes at shear stresses < 0.5 dyn/cm^2.

5. Conclusion

This is the first study, which shows that long, self-standing, biocompatible collagen hollow filaments with a diameter < 1000 μm can be directly extruded without supporting material. A collagen suspension containing natural grown fibres from porcine skin was used to fabricate the filaments. Other studies utilized collagen hydrogel reassembled from solution. Our technique led to higher mechanical stability and very low shrinkage of the collagen tubes during cell cultivation. ECs grown in the hollow channel of the filaments formed an endothelial layer with typical features of a healthy endothelium, suggesting that collagen hollow filaments support the biofunctionality of ECs. These observations demonstrated the suitability of the collagen hollow filaments for fabricating vascular tissue engineered constructs.

Declaration of interests

The authors declare that they have no known competing financial interests or personal relationships that could have appeared to influence the work reported in this paper.

Data availability

Data will be made available on request.

Supplementary materials

Supplementary material associated with this article can be found, in the online version, at doi:10.1016/j.bbiosy.2022.100067.

References

[1] Menager C, Vassy J, Doliger C, Legrand Y, Karniguian A. Subcellular localization of RhoA and ezrin at membrane ruffles of human endothelial cells: differential role of collagen and fibronectin. Exp Cell Res 1999;249(2):221–30.

[2] Perruzzi CA, Whelan MC, Senger DR, de Fougerolles AR, Koteliansky VE, Westlin WF. Functional overlap and cooperativity among αv and β1 integrin subfamilies during skin angiogenesis. J investigative dermatol 2003;120(6):1100–9.

[3] Montesano R, Orci L, Vassalli P. In vitro rapid organization of endothelial cells into capillary-like networks is promoted by collagen matrices. J Cell Biol 1983;97(5):1648–52.

[4] Sweeney SM, Guy CA, Fields GB, San Antonio JD. Defining the domains of type I collagen involved in heparin-binding and endothelial tube formation. Proceedings of the Nat Acad Sci 1998;95(13):7275–80.

[5] Whelan MC, Senger DR. Collagen I initiates endothelial cell morphogenesis by inducing actin polymerization through suppression of cyclic AMP and protein kinase A. J Biol Chem 2003;278(1):327–34.

[6] Onoe H, Okitsu T, Itou A, Kato-Negishi M, Gojo R, Kiriya D, Takeuchi S. Metre–long cell-laden microfibres exhibit tissue morphologies and functions. Nat Mater 2013;12(6):584–90.

[7] Gao G, Kim H, Kim BS, Kong JS, Lee JY, Park BW, Cho DW. Tissue-engineering of vascular grafts containing endothelium and smooth-muscle using triple-coaxial cell printing. Appl Phys Rev 2019;6(4):041402.

[8] Seliktar D, Black RA, Vito RP, Nerem RM. Dynamic mechanical conditioning of collagen-gel blood vessel constructs induces remodeling in vitro. Ann Biomed Eng 2000;28(4):351–62.

[9] Drzewiecki KE, Parmar AS, Gaudet ID, Branch JR, Pike DH, Nanda V, Shreiber DI. Methacrylation induces rapid, temperature-dependent, reversible self-assembly of type-I collagen. Langmuir 2014;30(37):11204–11.

[10] Diamantides N, Wang L, Pruiksma T, Siemiatkoski J, Dugopolski C, Shortkroff S, Bonassar LJ. Correlating rheological properties and printability of collagen bioinks: the effects of riboflavin photocrosslinking and pH. Biofabrication 2017;9(3):034102.

[11] Rhee S, Puetzer JL, Mason BN, Reinhart-King CA, Bonassar LJ. 3D bioprinting of spatially heterogeneous collagen constructs for cartilage tissue engineering. ACS Biomater Sci Eng 2016;2(10):1800–5.

[12] Lee ARHA, Hudson AR, Shiwarski DJ, Tashman JW, Hinton TJ, Yerneni S, Feinberg AW. 3D bioprinting of collagen to rebuild components of the human heart. Science 2019;365(6452):482–7.

[13] Covington AD. Tanning chemistry – the science of leather, skin and its components. Cambridge, United Kingdom: The Royal Society of Chemistry, RSC publishing; 2009. p. 134–6.

[14] Reing JE, Brown BN, Daly KA, Freund JM, Gilbert TW, Hsiong SX, Badylak SF. The effects of processing methods upon mechanical and biologic properties of porcine dermal extracellular matrix scaffolds. Biomaterials 2010;31(33):8626–33.

[15] Behrens S, Schmieder F, Polk C, Schöps P. PDMS free modular plug and play construction kit for the development of micro-physiological systems. Int Soc Optics and Photonics, Microfluidics, BioMEMS, and Medical Microsystems 2021;XIX(11637):116370O.

[16] https://www.elveflow.com/microfluidic-calculator/

[17] Buchanan CF, Voigt EE, Szot CS, Freeman JW, Vlachos PP, Rylander MN. Three--dimensional microfluidic collagen hydrogels for investigating flow-mediated tumor-endothelial signaling and vascular organization. Tissue Eng Part C: Methods 2014;20(1):64–75.

[18] Antons J, Marascio MGM, Aeberhard P, Weissenberger G, Hirt-Burri N, Applegate LA, Pioletti D. Decellularised tissues obtained by a CO2-philic detergent and supercritical CO2. European Cells and Mater 2018;36:81–95.

[19] Jung Y, Ji H, Chen Z, Chan HF, Atchison L, Klitzman B, Leong KW. Scaffold-free, human mesenchymal stem cell-based tissue engineered blood vessels. Sci Rep 2015;5(1):1–9.

[20] Fernandez CE, Yen RW, Perez SM, Bedell HW, Povsic TJ, Reichert WM, Truskey GA. Human vascular microphysiological system for in vitro drug screening. Sci Rep 2016;6(1):1–14.

[21] Alimperti S, Mirabella T, Bajaj V, Polacheck W, Pirone DM, Duffield J, Chen CS. Three-dimensional biomimetic vascular model reveals a RhoA, Rac1, and N-cadherin balance in mural cell–endothelial cell-regulated barrier function. Proceedings of the Nat Acad Sci 2017;114(33):8758–63.

[22] Gao G, Lee JH, Jang J, Lee DH, Kong JS, Kim BS, Cho DW. Tissue engineered bio-blood-vessels constructed using a tissue-specific bioink and 3D coaxial cell printing technique: a novel therapy for ischemic disease. Adv Funct Mater 2017;27(33):1700798.

[23] Singh A, Lee D, Sopko N, Matsui H, Sabnekar P, Liu X, Bivalacqua TJ. Biomanufacturing seamless tubular and hollow collagen scaffolds with unique design features and biomechanical properties. Adv Healthc Mater 2017;6(5):1601136.

[24] Itai S, Tajima H, Onoe H. Double-layer perfusable collagen microtube device for heterogeneous cell culture. Biofabrication 2018;11(1):015010.

[25] Li X, Xu J, Bartolák-Suki E, Jiang J, Tien J. Evaluation of 1-mm-diameter endothelialized dense collagen tubes in vascular microsurgery. J Biomed Mater Res Part B: Appl Biomat 2020;108(6):2441–9.

[26] Zeugolis DI, Paul RG, Attenburrow G. Engineering extruded collagen fibers for biomedical applications. J Appl Polym Sci 2008;108(5):2886–94.

[27] Haynl C, Hofmann E, Pawar K, Förster S, Scheibel T. Microfluidics-produced collagen fibers show extraordinary mechanical properties. Nano Lett 2016;16(9):5917–22.

[28] Tonndorf R, Aibibu D, Cherif C. Collagen multifilament spinning. Mater Sci Eng: C 2020;106:110105.

[29] Zhang Y, Yu Y, Akkouch A, Dababneh A, Dolati F, Ozbolat IT. In vitro study of directly bioprinted perfusable vasculature conduits. Biomater Sci 2015;3(1):134–43.

[30] Shen C, Zhang G, Wang Q, Meng Q. Fabrication of collagen gel hollow fibers by covalent cross-linking for construction of bioengineering renal tubules. ACS Appl Mater Interfaces 2015;7(35):19789–97.

[31] Oosterhoff LA, Kruitwagen HS, Van Wolferen ME, Van Balkom BW, Mokry M, Lansu N, Van Steenbeek FG. Characterization of endothelial and smooth muscle cells from different canine vessels. Front Physiol 2019;10:101.

[32] Meyer M. Processing of collagen based biomaterials and the resulting materials properties. Biomed Eng Online 2019;18(1):1–74.

[33] Sasaki N, Odajima S. Elongation mechanism of collagen fibrils and force-strain relations of tendon at each level of structural hierarchy. J Biomech 1996;29(9):1131–6.

[34] Buehler MJ. Nature designs tough collagen: explaining the nanostructure of collagen fibrils. Proceedings of the Nat Acad Sci 2006;103(33):12285–90.

[35] Salvatore L, Gallo N, Natali ML, Terzi A, Sannino A, Madaghiele M. Mimicking the hierarchical organization of natural collagen: toward the development of ideal scaffolding material for tissue regeneration. Front Bioeng Biotechnol 2021;9:258.

[36] Malda J, Klein TJ, Upton Z. The roles of hypoxia in the in vitro engineering of tissues. Tissue Eng 2007;13(9):2153–62.

[37] Magliaro C, Mattei G, Iacoangeli F, Corti A, Piemonte V, Ahluwalia A. Oxygen consumption characteristics in 3D constructs depend on cell density. Front Bioeng Biotechnol 2019;7:251.

[38] Place TL, Domann FE, Case AJ. Limitations of oxygen delivery to cells in culture: an underappreciated problem in basic and translational research. Free Radical Biol Med 2017;113:311–22.

[39] Cheema U, Rong Z, Kirresh O, MacRobert AJ, Vadgama P, Brown RA. Oxygen diffusion through collagen scaffolds at defined densities: implications for cell survival in tissue models. J Tissue Eng Regen Med 2012;6(1):77–84.

[40] Lo JH, Bassett EK, Penson EJ, Hoganson DM, Vacanti JP. Gas transfer in cellularized collagen-membrane gas exchange devices. Tissue Eng Part A 2015;21(15–16):2147–55.

[41] Bak SY, Lee SW, Kim KS, Kim HW. Physical and mechanical modifications of collagen microfibers using ethanol-based dehydrating conditions. Macromol Mater Eng 2016;301(11):1307–12.

[42] Bazzoni G, Dejana E. Endothelial cell-to-cell junctions: molecular organization and role in vascular homeostasis. Physiol Rev 2004;84(3):869–901.

[43] Tzima E, Irani-Tehrani M, Kiosses WB, Dejana E, Schultz DA, Engelhardt B, Schwartz MA. A mechanosensory complex that mediates the endothelial cell response to fluid shear stress. Nature 2005;437(7057):426–31.

[44] Conway DE, Breckenridge MT, Hinde E, Gratton E, Chen CS, Schwartz MA. Fluid shear stress on endothelial cells modulates mechanical tension across VE-cadherin and PECAM-1. Curr Biol 2013;23(11):1024–30.

[45] Davies PF. Hemodynamic shear stress and the endothelium in cardiovascular pathophysiology. Nat clin practice Cardiovasc med 2009;6(1):16–26.

[46] Garcia-Cardena G, Comander JI, Blackman BR, Anderson KR, Gimbrone MA Jr. Mechanosensitive endothelial gene expression profiles: scripts for the role of hemodynamics in atherogenesis? Ann N. Y. Acad Sci 2001;947(1):1–6.

[47] Chistiakov DA, Orekhov AN, Bobryshev YV. Endothelial barrier and its abnormalities in cardiovascular disease. Front. Physiol. 2015;6:365.

[48] Wang C, Baker BM, Chen CS, Schwartz MA. Endothelial cell sensing of flow direction. Arterioscler Thromb Vasc Biol 2013;33(9):2130–6.

[49] Baeyens N, Nicoli S, Coon BG, Ross TD, Van den Dries K, Han J, Schwartz MA. Vascular remodeling is governed by a VEGFR3-dependent fluid shear stress set point. Elife, 2015;4:e04645.

[50] Song JW, Daubriac J, Janet MT, Bazou D, Munn LL. RhoA mediates flow-induced endothelial sprouting in a 3-D tissue analogue of angiogenesis. Lab Chip 2012;12(23):5000–6.

[51] Vion AC, Perovic T, Petit C, Hollfinger I, Bartels-Klein E, Frampton E, Gerhardt H. Endothelial cell orientation and polarity are controlled by shear stress and VEGF through distinct signaling pathways. Front Physiol 2020;11:1743.

[52] Bosch-Rué E, Delgado LM, Gil FJ, Perez RA. Direct extrusion of individually encapsulated endothelial and smooth muscle cells mimicking blood vessel structures and vascular native cell alignment. Biofabrication 2020;13(1):015003.

[53] Dessalles CA, Leclech C, Castagnino A, Barakat AI. Integration of substrate-and flow-derived stresses in endothelial cell mechanobiology. Commun Biol 2021;4(1):1–15.